DHR51, the *Drosophila melanogaster* Homologue of the Human Photoreceptor Cell-Specific Nuclear Receptor, Is a Thiolate Heme-Binding Protein[†]

Eve de Rosny,[*,‡] Arjan de Groot,[⊥,‡] Celine Jullian-Binard,[‡] Franck Borel,[‡] Cristian Suarez,[‡] Laurent Le Pape,[§,||] Juan C. Fontecilla-Camps,[‡] and Hélène M. Jouve[‡]

CEA, CNRS, Université Joseph Fourier, UMR 5075, Institut de Biologie Structurale Jean-Pierre Ebel, 38027 Grenoble Cedex 1, France, CEA, CNRS, Université Joseph Fourier, UMR 5249, iRTSV, Laboratoire de Chimie et Biologie des Métaux, 38054 Grenoble, France, CEA, Université Joseph Fourier, UMR-E3, INAC, Laboratoire de Résonances Magnétiques, 38054 Grenoble, France

Received September 5, 2008; Revised Manuscript Received October 23, 2008

ABSTRACT: Heme has been recently described as a regulating ligand for the activity of the human nuclear receptors (NR) REV-ERBα and REV-ERBβ and their *Drosophila* homologue E75. Here, we report the cloning, expression in *Escherichia coli*, purification, and screening for the heme-binding ability of 11 NR ligand-binding domains of *Drosophila melanogaster* (DHR3, DHR4, DHR39, DHR51, DHR78, DHR83, HNF4, TLL, ERR, FTZ-F1, and E78), of unknown structure. One of these NRs, DHR51, homologous to the human photoreceptor cell-specific nuclear receptor (PNR), specifically binds heme and exhibits a UV−visible spectrum identical to that of heme-bound E75-LBD. EPR and UV−visible absorption spectroscopy indicates that, like in E75, the heme contains a hexa-coordinated low spin ferric iron. One of its axial ligands is a tightly bound cysteine, while the other one is a histidine. A dissociation constant of 0.5 μM for the heme was measured by isothermal titration calorimetry. We show that DHR51 binds NO and CO and discuss the possibility that DHR51 may be either a gas or a heme sensor.

Nuclear receptors (NR[1]), the largest superfamily of transcriptional regulators in metazoans, regulate transcription through the binding of small hydrophobic hormones. They are involved in critical physiological processes such as homeostatic control of energy and glucose levels, lipid metabolism, detoxification, cellular differentiation, circadian clock, and embryonic development. Mutations in NR genes or chronic ligand excess are associated with human disorders such as cancer, diabetes, or heart diseases (*1*). NRs contain a highly conserved DNA binding domain (DBD) and a less conserved ligand-binding domain (LBD) connected by a flexible hinge. Typically, binding of the ligand to LBD induces conformational changes that both trigger release of a corepressor protein and promote binding of a coactivator protein to initiate transcription. However, other regulating mechanisms have been observed. The C-terminal AF-2 activation domain, which is involved in the binding of the coactivator and the corepressor, also forms a major interface for dimerization of the NRs (*2, 3*).

NRs are classified according to their DBD sequence into six phylogenic subfamilies. The *Drosophila melanogaster* genome encodes 18 NRs distributed into the 6 subfamilies (*4*), but only the LBD crystal structures of USP, EcR, DHR38, and FTZ-F1 have been reported for this insect (*5*−*7*). Most of *D. melanogaster* NRs are considered to be orphan, meaning that their natural ligand, if it indeed exists, has not been identified. Nevertheless, three ligands have been identified so far: the key hormone 20-hydroxyecdysone, which binds to EcR and forms the active ecdysone/EcR/USP complex that directs the expression or repression of E75, E78, DHR3, FTZ-F1, DHR39, and DHR4 involved in embryonic development; the juvenile hormone, which has been proposed to bind USP, but the biological relevance of the resulting complex was not clearly established; and heme, which we and others have shown to bind to E75 (*8, 9*) and that plays a role in transcription regulation.

In vivo, E75 binds to DHR3 and inhibits its activating function on the *FTZF-1* promoter (*10*). E75 is very likely a gas sensor because CO prevents its binding to a DHR3-derived peptide corresponding to the AF-2 activation domain and *in vitro* transcription experiments showed that NO blocks E75 repressor activity (*8*). In addition, two recent publications (*11, 12*) showed that heme is required for the repressor activity of the human E75 homologues REV-ERBα and REV-ERBβ. Recently, the crystal structure of REV-ERBβ in a complex

[†] This work was supported by Genopole Rhone-Alpes.

* Corresponding author. LCCP, Institut de Biologie Structurale (UMR 9015), 41 rue Jules Horowitz 38027 Grenoble Cedex 1, France. Tel: 33 (4) 3878 5924, Fax: 33 (4) 3878 5494. E-mail: eve.derosny@ibs.fr.

[‡] Institut de Biologie Structurale Jean-Pierre Ebel.

[§] Laboratoire de Chimie et Biologie des Métaux.

[||] Laboratoire de Résonances Magnétiques.

[⊥] Current address: CEA, DSV, IBEB, SBVME, UMR 6191 CNRS/CEA/Aix Marseille Univ, Saint Paul Lez Durance, F-13108 France.

[1] Abbreviations: NR, nuclear receptor; DBD, DNA binding domain; LBD, ligand-binding domain; LXR, liver X receptor; PNR, photoreceptor cell-specific nuclear receptor; EcR, ecdysone receptor; DHR, *Drosophila* hormone receptor; USP, ultraspiracle; PPAR, peroxisome proliferator-activated receptor; RXR, retinoid X receptor; ERR, estrogen receptor-related receptor; FTZ-F1, *fushi tarazu*-factor 1; HNF4, hepathocyte nuclear factor 4; TLL, Tailless; DSF, dissatisfaction; SVP1, seven-up; UV, ultraviolet; EPR, electron paramagnetic resonance; Rz, Reinheitszahl index; IAM, iodoacetamide; NEM, *N*-ethylmaleimide; ITC, isothermal titration calorimetry; HSA, human serum albumin; DHR51-LBD, His6 tagged LBD of DHR51.

10.1021/bi801691b CCC: $40.75
Published on Web 11/14/2008

with heme has been deposited in the Protein Data Bank (PDB ID: 3CQV). In that high-resolution structure, the heme iron is coordinated, in the ligand-binding pocket, by a histidine and a cysteine. The same coordination takes place in E75 (*8, 9*).

In this article, we have explored the heme binding ability of several *D. melanogaste*r nuclear receptors and demonstrate that DHR51-LBD, whose gene (*cg16801*) was annotated in the *D. melanogaster* genome as coding for a NR (*13*), binds heme in the same way E75 does. Also, the reduced heme iron binds NO and CO. DHR51 is the homologue of the orphan human photoreceptor cell-specific nuclear receptor (PNR) that controls neuronal differentiation in the developing retina (*14*).

MATERIAL AND METHODS

Cloning, Protein Expression, and Purification. pSKB3 clones encoding the LBDs from DHR3, DHR39, and FTZ-F1 were gifts from J. P. Renaud and Claude Dauer (Strasbourg, France). They were generated as previously mentioned (*9*). The other LBD clones, namely, DHR4, DHR51, DHR78, DHR83, DHR96, HNF4, TLL, ERR, SVP-1, DSF, and E78, were obtained as follows. RNAs from third instar larva, prepupae, and pupae were isolated using the RNeasy Mini Kit (Qiagen). Twenty-five insects per Eppendorf tube were frozen and stored at −80 °C prior to RNA isolation. They were subsequently disrupted using a pestle for Eppendorf tubes, followed by homogenization of the lysate using a QIA shredder. The LBD-encoding cDNA for each NR was obtained by RT-PCR using the Superscript One-Step RT-PCR with Platinum *Taq* system (Invitrogen), oligonucleotides specific for each NR (Supporting Information, Figure S1), and 1 μg of total RNA per reaction. cDNA fragments were cloned in a pCR2.1-TOPO vector (Invitrogen) and verified by sequencing; *cg7404* (encoding ERR) was then cloned in pET 28a, whereas all of the other LBDs were cloned in pSKB3 (a gift from J. P. Renaud, Strasbourg, France), using the appropriate restriction sites. Expression and purification of the His6-tagged NRs were performed as previously described (*9, 15*). Hemin was purchased from Sigma-Aldrich.

Heme Binding to Human Serum Albumin (HSA) As a Scaffold Protein. The experiment was performed in 50 mM Tris-HCl buffer and 300 mM NaCl at pH 8. Hemin was added to HSA (purchased from Sigma-Aldrich) at substoichiometric concentrations (1:3 molar ratios) to avoid the presence of free hemin in the solution. The resulting UV−visible spectrum, with a peak at 402 nm, was typical of the reported heme−HSA complex (*16*). NRs and HSA were incubated 10 min before purification on a cobalt column (Talon, Clontech). The HSA was eluted with 50 mM Tris-HCl (pH 8.5) and 300 mM NaCl; the NR was eluted with 50 mM Tris-HCl (pH 8.5), 300 mM NaCl, and 300 mM imidazole.

Cleavage of the His6-Tag. The His6-tag of DHR51-LBD was cleaved by adding 3 μL of His6-Tev protease (acTEV, Invitrogen) to 800 μL of 15 μM DHR51-LBD in 50 mM Tris and 300 mM NaCl (pH 8.5). The cleaved solution was then purified by batch chromatography. This procedure was used because column purification resulted in an unstable form of the protein. Cleavage and purification of untagged protein was confirmed by SDS−PAGE and Western blotting with anti·His-HRP conjugates (Sigma-Aldrich).

Isothermal Titration Calorimetry (ITC). The ITC experiments were carried out using a MicroCal VP-ITC titration microcalorimeter (Northampton, MA). The titration was performed in 50 mM Tris-HCl buffer, 25 mM NaOH, and 25 mM NaCl at a final pH of 8.0. The reaction cell (V = 1.4478 mL) contained a solution of 0.031 mM DHR51-LBD. Thirty 10 μL-aliquots of 0.294 mM hemin were successively injected to the protein solution at 4-min intervals using a computer-controlled 300 μL microsyringe. The solution was stirred at 300 rpm while kept at 25 °C. Both DHR51-LBD and hemin solutions were thoroughly degassed by stirring under vacuum before titration. Because of hemin adsorption, the calorimetric cell and the microsyringe used for injections were extensively washed after each experiment. The amount of heat produced per injection was calculated by integrating the area under the individual peaks with the instrument software. The enthalpy change (H), the association constant (K_a), and the stoichiometry of the interaction (i.e., number of binding sites per receptor) were calculated by fitting the experimental data to a theoretical titration curve using the ORIGIN software (MicroCal)) and the one set of binding sites model. The dissolution heat of the ligand was measured by injecting hemin into the buffer alone and was subsequently subtracted from the reaction heat in order to obtain the effective heat produced upon complex formation. Standard deviations were calculated by averaging two independent experiments.

Competition Assay with HasA. The HasA protein was a gift from Nadia Izadi-Pruneyre (Unité des Membranes Bactériennes, CNRS URA 1300, Institut Pasteur, Paris, France). Both heme-bound DHR51-LBD and E75-LBD were incubated at room temperature, in 50 mM Tris buffer and 300 mM NaCl at pH 8.0, with a slight molar excess of apo-HasA.

Optical Absorption Spectra and EPR. The optical spectra were routinely recorded at room temperature under air with a Carry 50 UV−visible spectrophotometer and in a glovebox with a PC-2000 spectrophotometer/DH-2000-BAL light source (Ocean Optics). The concentration of the His6-tagged apo-DHR51-LBD was calculated using the extinction molar coefficient ε_{280} = 27.305 M^{-1} cm^{-1}, at 280 nm, obtained from the amino acid sequence. Continuous-wave (CW) X-band EPR spectra were recorded on a Bruker EMX spectrometer equipped with an Oxford Instruments ESR 900 helium flow cryostat and an ER-4116 DM Bruker cavity. Samples were introduced in a synthetic Suprasil quartz EPR tube under argon. For the oxidized form of DHR51, 8% (v/v) glycerol was added to the sample, as a cryoprotectant. For the NO-bound, reduced form of DHR51, the simulation was performed with the EPR program (F. Neese, Germany) using the spin Hamiltonian (eq 1) considering collinear $\tilde{g}$ and $\tilde{A}$ tensors.

$$H = \mu_B B \cdot \tilde{g} \cdot S + S \cdot \tilde{A} \cdot I \quad (1)$$

with B being the magnetic field, S = 1/2, and I = 1. Because of the lack of resolution, A_1 and A_2 were fixed at 0.

Modification of DHR51 Histidines with Diethylpyrocarbonate. Diethylpyrocarbonate (DEPC) (Sigma-Aldrich) was prepared by fresh dilution of the reagent in ethanol. DEPC

reacted with apo- and heme-bound DHR51-LBD. In the first case, purified DHR51-LBD in 50 mM Tris (pH 8.5) and 300 mM NaCl was diluted in 50 mM phosphate (pH 6.5) prior to the addition of DEPC at 200-fold molar excess. Unbound reagent was removed by gel-filtration chromatography on a micro-biospin6 column (Biorad), equilibrated with potassium-phosphate (pH 8.0). The concentration of the eluted protein was calculated from its absorbance at 280 nm before the addition of a stoichiometric concentration of heme. In the second experiment, hemin was added to concentrated DHR51-LBD in 50 mM Tris (pH 8.5) and 300 mM NaCl at a 1:1 molar ratio. Heme-bound DHR51-LBD was diluted in 50 mM potassium-phosphate (pH 6.5) before the addition of the DEPC reagent at 200-fold molar excess. The reaction product was then gel-filtered on a micro-biospin6 column equilibrated with 50 mM potassium phosphate (pH 8.0).

Reduction of the Heme Iron and Binding of NO and CO. The heme iron was reduced by the addition of dithionite (100 mM in 0.1 M NaOH) to the heme-bound DHR51-LBD solution (in 50 mM Tris (pH 8.0) and 300 mM NaCl), at room temperature in an anaerobic chamber. The NO gas was generated by a 100-fold dilution of diethyamine NONOate purchased from Cayman (100 mM in 10 mM NaOH) in 50 mM Bis-Tris (pH 6.5). This NONOate preparation was gradually added to the Fe(II)-heme containing DHR51-LBD in solution. The saturation of the heme by NO was followed by absorption spectroscopy. Fe(II)-CO was generated by a 2-fold dilution of the Fe(II) DHR51-LBD solution with 50 mM Tris (pH 8.0) and 300 mM NaCl previously bubbled with pure CO.

RESULTS

Nuclear Receptor Cloning and Expression. The cDNAs encoding the hinge region and the LBD (DE domain) of DHR4, DHR51, DHR78, DHR83, DHR96, HNF4, TLL, ERR, SVP-1, DSF, and E78 were cloned as described in Materials and Methods. Their translated sequences were identical to the corresponding *D. melanogaster* gene sequences in databases, except for DHR51 and DHR83. The cloned DHR51 sequence, especially the hinge region, more closely resembles the predicted amino acid sequence of GA14159 from *Drosophila pseudoobscura* than the reported sequence of the *D. melanogaster* NR (CG16801-PB; A1ZA01_DROME) (Supporting Information, Figure S2). Likewise, our cloned DHR83 sequence contained two residues that are different from those reported for the *D. melanogaster* protein (CG10296-PA; Q9VI12_DROME) but are conserved in related NR sequences and in the *D. pseudoobscura* homologue (Supporting Information, Figure S3). The discrepancies between our sequences and the ones predicted for *D. melanogaster* might result from errors in fruit fly genome sequencing or variations from strain to strain. It is noteworthy that two slightly different sequences of DHR4 were present in databanks; our cloned sequence corresponds to the AL035245 DNA accession number. The NR LBDs from DHR4, DHR51, DHR78, DHR96, E78, HNF4, SVP1, and DSF were also cloned without the hinge region (E domain) and expressed in *E. coli* (Supporting Information, Figure S4). Ten of the NR LBDs were soluble and could be purified, whereas DHR96, SVP-1, DHR4, and DSF were expressed as inclusion bodies. In a previous work, we mutated a putative Phe surface residue of E75-LBD to Tyr in order to obtain soluble protein (*9*).

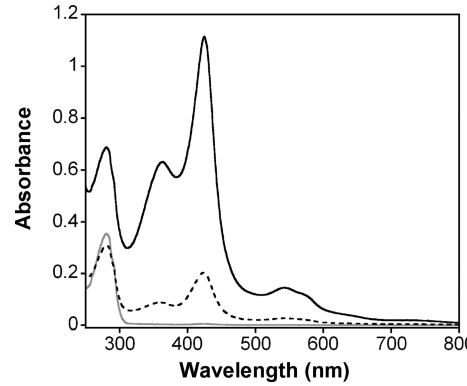

FIGURE 1: Effect of heme binding on the UV−visible spectra of DHR51. Thirteen micromolar of apo-DHR51 (gray line) was incubated with a 1:1 molar ratio of hemin (black line). Heme bound DHR51 was also generated by mixing of apo-DHR51 (68 μM) with heme bound HSA (226 μM); the nuclear receptor was subsequently separated from HSA on a cobalt column, which resulted in its dilution (broken line). Experimental conditions: 50 mM Tris, pH 8.0, and 300 mM NaCl. The spectra were recorded at room temperature.

Table 1: Position of the Electronic Absorption Peaks (nm) of Heme Bound DHR51-LBD

DHR51	δ	Soret	visible
Fe^{3+}(hemin)	362	424	542, 575
Fe^{2+}(heme)		424	531, 560
Fe^{2+}(heme)-NO		391	536, 566
Fe^{2+}(heme)-CO		420	521, 566

Heme Incorporation to the Drosophila Nuclear Receptors. To test their ability to bind heme, *D. melanogaster* NR LBDs were expressed in *E. coli*, in the presence of added hemin, as previously described (*9*). The absence of a peak in the visible range of the absorption spectra after purification on a cobalt column showed that the LBD of DHR3, DHR39, DHR78, ERR, FTZ-F1, E78, and TLL did not bind heme under our experimental conditions. However, DHR83, HNF4, and DHR51 LBDs exhibited peaks at 418 nm, 415, and 424 nm, respectively, with A_{Soret}/A_{280} ratios less or equal to 0.3 (data not shown), indicating that although they can bind heme, the binding is much weaker than E75, which displays a A_{Soret}/A_{280} ratio of 2.4 (*9*) under the same conditions.

When expressed in the absence of hemin, purified DHR51-LBD did not exhibit the Soret band (Figure 1, gray line). Addition of a stoichiometric concentration of hemin to apo-DHR51-LBD produced a spectrum with four new peaks: a δ-peak at 362 nm, a γ-peak at 424 nm, a β-peak at 542 nm, and an α-peak at 575 nm (Figure 1, black line and Table 1). This spectrum, which exhibits a A_{Soret}/A_{280} ratio of 1.6, is typical of hemoproteins and indicates that heme was incorporated to the DHR51-LBD. Furthermore, the spectrum is identical to that of the E75-LBD (*9*), which, in turn, strongly suggests a similar coordination of the heme iron in the two NRs. The absence of vitamin B12 and protoporphyrin IX binding to the purified DHR51-LBD confirmed the specificity of heme binding (data not shown). Depending on the sample, the presence of a small CT-1 band at 645 nm was sometimes detected. This band indicated the presence of a high spin species, as confirmed by EPR, and probably reflects the instability of heme iron binding to one of its axial

ligands (data not shown). However, the addition of a 0.5 mol equiv of hemin to apo-DHR83 and HNF4 LBDs resulted in poorly resolved spectra, probably reflecting the presence of both bound heme and free hemin and therefore a weaker affinity of these NRs when compared to the one for DHR51 under the same experimental conditions (Supporting Information, Figure S5A).

To test whether the NRs affinity for heme was higher when supplied from a scaffold protein, the heme−HSA complex was added to the NR LBDs at a 3:1 molar ratio. Subsequently, the NRs were separated from HSA on a cobalt column prior to measuring the UV−visible spectra. DHR83-LBD and HNF4-LBD exhibited Soret bands at 410 nm with A_{Soret}/A_{280} ratios of 0.46 and 0.47, respectively (Supporting Information, Figure S5B). DHR51-LBD exhibited its characteristic Soret band at 425 nm with an A_{Soret}/A_{280} ratio of 0.65 (Figure 1B, broken lines). Addition of stoichiometric concentrations of heme-HSA to the NRs resulted in A_{Soret}/A_{280} ratios of 0.18, 0.13, and 0.52 for DHR83, HNF4, and DHR51 LBDs, respectively (data not shown). These binding experiments with HSA-bound hemin confirmed that DHR83 and HNF4 LBDs bind heme (but with a significantly lower affinity than DHR51) and show that the affinity did not increase when heme was delivered by a carrier protein.

The His6-tag of DHR51-LBD was cleaved by His6-Tev protease (acTEV, Invitrogen) and purified by cobalt batch chromatography (see Materials and Methods). We verified, using circular dichroism, that the His6-tag neither significantly modified the ellipticity content of the protein, nor did it change its thermal shift transition (Supporting Information, Figure S6A and B). When 0.3 mol equiv of hemin was added to the cleaved protein, the resulting UV−visible spectrum exhibited a Soret band at 421 nm corresponding to a 3 nm blue shift relative to the uncleaved protein. However, the A_{Soret}/A_{280} ratio was not modified (Supporting Information, Figure S6C). However, cleavage of the His6-tag on heme-enriched DHR51-LBD did not change the Soret band position, which remained at 424 nm (data not shown). In both cases, the absence of a CT-1 band at 645 nm indicates that there is no significant modification of the iron coordination that could generate high-spin species. Taken together, these results show that the His6-tag is not directly involved in heme iron coordination. However, the tag may slightly modify the orientation of the amino acids involved in iron coordination, leading to a shift of the Soret band.

Thermodynamic Profile of Heme Binding. The thermodynamic parameters of heme binding were determined using ITC (Figure 2). Apo-DHR51-LBD bound hemin with a K_a of 2.3(±0.3) μM^{-1} ($K_d = 0.43\ \mu M$). The process is clearly enthalpy driven since the corresponding free energy $\Delta G = -36$ kJ/mol has an enthalpy contribution $\Delta H = -31 \pm 1$ kJ/mol. The entropy contribution is favorable but very limited, with $T\Delta S = 5$ kJ/mol. The stoichiometry of 0.75 ± 0.03 is consistent with the UV−visible absorption data of heme binding and is the signature of one binding site per DHR51-LBD molecule.

Comparison of Heme Affinity and Heme Accessibility in E75 and DHR51. Because apo-E75-LBD was not able to incorporate heme after purification (*9*), its affinity for heme could not be determined by microcalorimetry. Thus, in order to compare E75-LBD and DHR51-LBD affinity for this ligand, the stability of heme binding was tested using the bacterial hemophore HasA. This protein takes up heme from hemoproteins such as hemoglobin with a $K_d = 2.0 \times 10^{-11}$ M and shuttles it to specific receptors (*17*). After incubation of the apo form of HasA with heme-containing His6-tagged DHR51 or E75 LBDs, the UV−visible spectra of the two LBDs were dramatically changed. The resulting spectra were characteristic of the HasA holo-form (*18*) with a Soret band at 407 nm and four other peaks at 492, 538, 568, and 617 nm (Figure 3; Supporting Information, Figure S7). These results show that HasA took up the heme from both NR

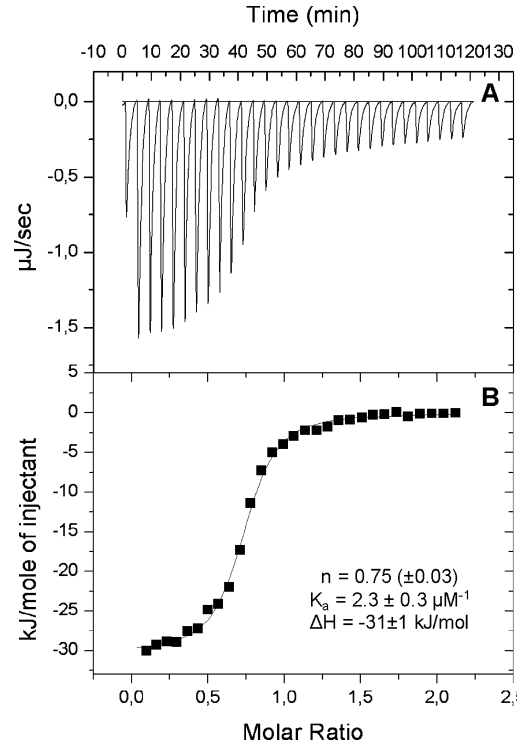

FIGURE 2: Isothermal titration of DHR51 with hemin. The ITC experiment was carried out at 25 °C in 50 mM Tris-HCl, 25 mM NaOH, and 25 mM NaCl at pH 8.0 using 0.031 mM apo-DHR51-LBD. (A) Isothermal traces for a series of 10 μL injections of 0.294 mM hemin. (B) Integrated heat signals (squares) after subtracting the heat of hemin dilution into the buffer in the absence of protein. Heat signals (integrated values in microcalories per second per injection) are fitted to a single-binding model.

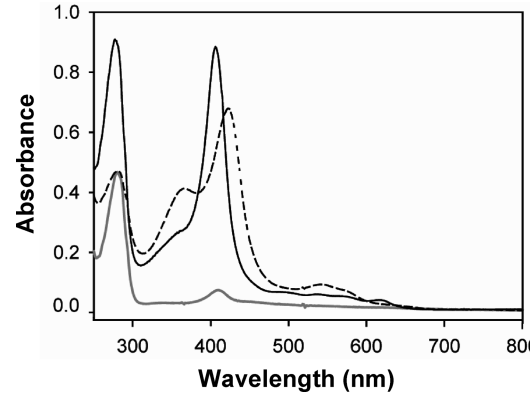

FIGURE 3: Effect of apo-HasA on the UV−visible spectrum of DHR51. Heme-bound DHR51-LBD (6.5 μM) was rapidly mixed with 18 μM apo-HasA and incubated about 5 min at room temperature before recording the UV−visible spectrum (black line). Reference spectra of separated proteins before mixing: 6.5 μM heme-containing DHR51-LBD (broken line) and 18 μM apo-HasA (gray line).

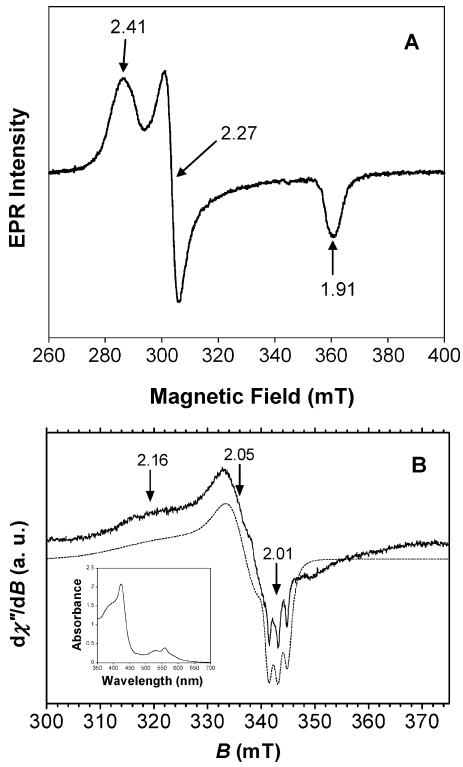

FIGURE 4: X-Band EPR spectra. (A) Heme-saturated DHR51-LBD (120 μM) in the g$\sim$2 region at 13 K. Experimental conditions: 50 mM Tris-HCl, 300 mM NaCl, and 8% (v/v) glycerol (pH 8.0); modulation frequency, 100 kHz; modulation amplitude, 1 mT; microwave power, 1 mW. (B) DHR51-LBD (50 μM) in the presence of 95 μM NONOate at 50 K, with simulation depicted as a dotted line; microwave frequency, 9.655 GHz; microwave power, 12.6 mW; modulation frequency, 100 kHz; modulation amplitude, 0.3 mT; time constant, 41 ms using 21 scans (1 h). Simulation obtained with $g_1 = 2.160$ (5), $g_2 = 2.053$ (2), $g_3 = 2.012$ (1); $A_1 = A_2 = 0$, $A_3 = 50$ (3) MHz; $W_1 = 10$ (2) mT, $W_2 = 3.0$ (5) mT, $W_3 = 0.60$ (2) mT; inset, absorption spectra of the sample. Buffer conditions: 50 mM Tris-HCl (pH 8.5) and 300 mM NaCl.

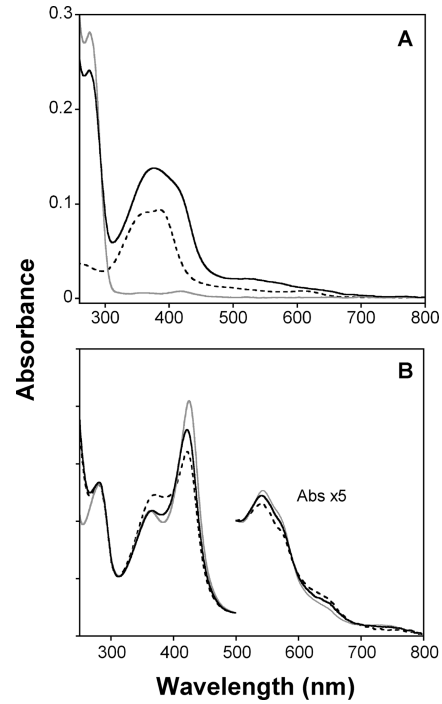

FIGURE 5: Spectral analysis of DHR51 modified by DEPC. (A) DHR51-LBD (30 μM) was incubated with 6.0 mM DEPC in 50 mM potassium-phosphate (pH 6.5), then filtrated on a desalting gel column equilibrated with potassium-phosphate (pH 8.0) buffer (gray line) before the addition of a 1:1 molar ratio of hemin to the resulting protein solution (10 μM, black line); free hemin (1.6 μM, broken line). (B) DHR51-LBD (30 μM) was incubated with a stoichiometric concentration of hemin at pH 8.0 then diluted 10 times in 50 mM potassium-phosphate at pH 6.5 (gray line); 0.6 mM DEPC was added before gel filtration (broken line) and the addition of 10 mM imidazole (black line); spectra are normalized relative to the 280 nm absorption peak. The reactions were carried out at room temperature.

LBDs. The rate of heme dissociation was much higher for DHR51-LBD than for E75-LBD. Heme extraction was completed in less than 5 min for DHR51-LBD, whereas it took more than 10 h for E75-LBD (Supporting Information, Figure S7C). However, apo-HasA could not extract the completely buried heme from *Proteus mirabilis* catalase ((*19*), data not shown), suggesting that despite its high stability (*8*) the heme in E75-LBD and DHR51-LBD is, at least partially, accessible to solvent. The slow rate of heme displacement also indicates that E75 and HasA have relatively similar affinities for heme. Consequently, the K_d value of the former can be estimated to be in the nanomolar range. The high rate of heme extraction observed with DHR51-LBD is consistent with the affinity in the micromolar range measured by ITC.

Iron Ligand Characterization. As in the case of E75-LBD, the EPR spectrum of DHR51-LBD exhibited broad line widths, reflecting heterogeneity in iron coordination. The average *g* values of 2.41, 2.27, and 1.91 (Figure 4A) correspond to a low-spin ferric iron. Theses *g* values are in the range found for thiolate hemoproteins (*20*). However, because the EPR spectrum in Figure 4A is compatible with either O-, N-, or S- donor atoms trans to the cysteine iron ligand (*21*−*23*), it is not possible to establish the nature of the second axial ligand. The participation of a cysteine thiolate iron ligand was confirmed by the treatment of DHR51-LBD with either IAM or NEM. Modification of the cysteine thiolates prior to hemin addition prevented heme incorporation, whereas modification of the cysteine thiolates after hemin addition did not result in heme release (data not shown). These results indicate that the axial cysteine thiolate is strongly coordinated to the Fe(III) heme iron and cannot be displaced by a thiol-specific reagent.

On the basis of the very similar UV−visible absorption spectra of DHR51-LBD and E75, we investigated the possibility of a histidine ligand trans to the cysteine in the former. The apo and heme-bound forms of DHR51-LBD were treated with diethylpyrocarbonate (DEPC). Chemical modification by DEPC was shown to induce heme release in histidine-coordinated hemoproteins (*24, 25*). Modification of the DHR51-LBD histidine side chains was followed by measuring the increase in absorbance at 240 nm (*26*), and it was achieved for a DHR51-LBD/DEPC molar ratio of 1:200. Addition of DEPC to apo DHR51-LBD prevented heme binding as shown by the poorly resolved spectra, which resemble that of free heme (Figure 5A). However, addition of DEPC to heme-bound DHR51-LBD did not result in heme release, as indicated by the spectrum shown in Figure 5B (broken line), which is characteristic of a hemoprotein. However, there were significant spectral changes upon modification of the histidines: the Soret band was slightly blue-shifted to 421 nm with a 22% decrease in intensity;

```
  E75  .......... .TELDDQPRL LAAVLRAH.L ETCEFTKEKV SAMRQRARDC
DHR51  IDPSSPAPEN AKEKNIAGGS VSSVSSSSPT MENDNDDDSI DVTNDNEEPH
       .......... ..E....... ...V...... .......... ..........

                  *
  E75  PSYSMPTLLA CPLNPAPELQ SEQEFS..QR FAHVIRGVID FAGMIPGFQL
DHR51  AVSRSDSSFI MPQFMSPNLY THQHETVYET SARLLFMAVK WAKNLPSFAR
       .......... .P....P.L. ..Q....... .A..L..... .A...P.F..

                                          *
  E75  LTQDDKFTLL KAGLFDALFV RLICMFDSSI NSIICLNGQV MRRDAIQNGA
DHR51  LSFRDQVILL EESWSELFLL NAIQWCIPLD PTGCALFSVA EHCNNLENNA
       L...D...LL .......... ..I....... .....L.... .......N.A

  E75  NARFLVDSTF NFAE...... ...RMNSMNL TDAEIGLFCA IVLITPDRPG
DHR51  NGDTCITKEE LAADVRTLHE IFCKYKAVLV DPAEFACLKA IVLFRPETRG
       N......... ..A....... .......... ..AE.....A IVL..P...G

                                                    *
  E75  LRNLELIEKM YSRLKGCLQY IVAQNRPDQP EFLAKLLETM PDLRTLSTLH
DHR51  LKDPAQIENL QDQAHVMLSQ HTKTQFTAQI ARFGRLLLML PLLRMISSHK
       L.....IE.. .......L.. ........Q  .....LL... P.LR..S...


  E75  TEKLVVFRTE HKELLRQQMW SMEDGNNSDG QQNKS
DHR51  IESIYFQRTI GNTPMEKVLC DMYKN..... .....
       .E.....RT. .......... .M........ .....
```

FIGURE 6: Sequence alignment of DHR51 and E75 LBDs created using the MultiAlign sequence alignment server. Asterisks denote the position of the amino acid residues of E75 involved in the heme iron coordination, C368, C396, and H574 (*9*). Residues conserved in nuclear receptors are highlighted in red (100%), yellow (>80%), and gray (>60%) according to Brelivet et al. (*49*).

the δ band was red-shifted from 362 to 366 nm, and its intensity increased, and the CT-1 band at 645 nm also increased, reflecting the conversion of a low spin to a high spin heme species. Addition of imidazole to this modified heme-bound DHR51-LBD resulted in a spectrum very similar to that of the native protein (Figure 5B black and gray lines). The main differences with the former were a Soret band at 421 nm; a 12.5% reduction of the Soret band intensity; a less pronounced valley at 380 nm; and the remaining of a higher CT-1 band, as compared to unmodified DHR51-LBD. These observations suggest that imidazole binds, at least partially, to the heme iron at the axial site, which became accessible after chemical modification of the histidine side chains. These data also reveal that modification by DEPC precluded the binding of a histidine iron ligand trans to the cysteine ligand. This interpretation is strengthened by the shape of the absorption spectrum of DEPC-modified heme-bound DHR51-LBD that has an absorbance spectrum very similar to the one of the E75 H74A mutant (*9*).

The amino acid sequence alignment between the DHR51 and E75 LBDs (Figure 6) indicates that there is one histidine located one position ahead of H574 that in E75-LBD was shown to be an axial ligand of the heme iron (*9*). However mutation of the corresponding DHR51 histidine residue to alanine did not modify heme binding (data not shown), which indicates that this histidine is unlikely involved in heme binding.

Spectral Analysis of DHR51 Reduced and in Complex with NO and CO. The Soret band position (424 nm) was not modified by the addition of dithionite even though the two new peaks, α at 531 nm and β at 560 nm, confirm that the reduction took place (Figure 7, gray line and Table 1). Comparison of these peak positions with those of other heme-thiolate proteins strongly suggests that, in this hexa-coordinated reduced form, the cysteine ligand is replaced

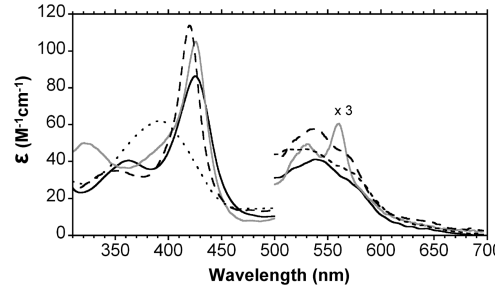

FIGURE 7: Spectral analysis of DHR51, oxidized, reduced and in complex with NO and CO. UV−visible spectra at room temperature of DHR51-LBD containing Fe(III) (12 μM, black line), Fe(II) (11 μM of Fe(III) DHR51-LBD and 10 mM dithionite, gray line), Fe(II)-NO (11 μM Fe(II) and 125 μM NONOate, dotted line), or Fe(II)-CO (7 μM Fe(II) and dissolved CO gas, broken line). ε, molar absorption. From 500 to 700 nm, the ordinate axis is increased 3-fold.

by a neutral residue. Proteins undergoing such redox-mediated ligand switching exhibit, in their reduced form, Soret bands around 420 nm (*27*). On the contrary, hCBS at pH 9 or P450-CAM, which keeps its cysteine bound to iron, exhibits Soret bands around 450 nm (*28, 29*).

Addition of CO shifted the Soret band of Fe(II)-DHR51 from 424 to 420 nm (Figure 7, broken line and Table 1). The position of the Soret band, far from 450 nm, indicates that DHR51-LBD is not a cytochrome P450-like hemoprotein and does not have a cysteinate trans to the CO. It belongs to the other heme-thiolate class, in which the peak around 420 nm was shown to reflect the presence of a neutral amino acid trans to the CO. This neutral residue, presumably a histidine like in CooA, HRI, and NPAS2 (*30*−*32*), may also be a methionine, a proline, or even a neutral thiol as proposed by Perera et al. (*33*).

Addition of NO shifted the Soret band to 391 nm (Figure 7, dotted line and Table 1), indicating the presence of a five-

coordinated NO-heme. The loss of two protein axial ligands was confirmed by EPR spectroscopy. NO was generated using a NONOate compound at a concentration leading to half-saturation of the axial binding site of the heme iron (Figure 4B, inset). An EPR signal was observed close to $g = 2$ (Figure 4B). It was under saturation at 50 K and 12.6 mW. No other signal was detected from 5 to 900 mT (data not shown). The signal shape indicates the binding of NO to the low-spin Fe(II) heme (*34, 35*). The three resolved hyperfine lines centered at $g = 2.012$ are due to the nitrogen nuclear-spin $I = 1$ of NO. Super hyperfine lines, expected if the N-donor histidine were still bound as a sixth ligand trans to the NO, were not observed. The simulation gave additional evidence of a five-coordinated heme iron. The values of g_1 (2.160), g_2 (2.053), g_3 (2.012), and A_3 (50 MHz) reveal that $g_2 > 2.005$, $g_3 > 1.979$, $g_{average} > 2.019$, and $A_3 < 56$ MHz, characteristic of a five-coordinated nitrosyl heme (*34, 36*).

The O_2 complex could not be detected by UV−visible spectral analysis because of the very high auto-oxidation rate of the heme iron.

DISCUSSION

Nuclear receptors are involved in almost all physiological processes, typically modulated by their binding to small hydrophobic molecules. However, the majority of nuclear receptor ligands have not been identified. Discovery of new NR ligands has therefore profound implications for our understanding of biological mechanisms. Heme, along with its many other functions, is a regulator of protein expression. It plays the role of the signaling ligand in proteins such as Hap1, Bach1, and HRI (*37*), or it binds diatomic gas molecules in gas-sensor proteins such as CooA (*38*). Recently, heme was found to bind and to regulate the activity of the *Drosophila* nuclear receptor E75. It was therefore logical to investigate the heme as the ligand of the other *Drosophila* nuclear receptors.

Our systematic study reported here showed that three of the 10 NRs that were successfully expressed and purified from *Escherichia coli* incorporated heme. The weak affinity of HNF-4 and DHR83 for heme (both free and bound to a scaffold protein), when compared to the μM−nM range typically found with other nuclear receptors for their cognate ligand, suggests that heme is not their natural ligand. However, we cannot rule out that their affinity for heme is higher in the full-length protein and in the cell. The natural ligand of HNF-4 of *Drosophila* has not been characterized, but many data suggest that, like its mammalian homologues HNF-4α and HNF-4γ, it is involved in lipid metabolism and in vivo probably binds lipids (*39*). DHR83, like its closest homologue DHR51, was only recently discovered, and its function remains unknown. Nevertheless, because of their poor binding affinity to heme, we did not investigate the heme iron coordination of these two nuclear receptors any further.

However, DHR51-LBD binds heme with a K_d of 0.43 μM. Most NR-ligand K_d values fall in the nanomolar range (as is the case for E75), but micromolar range values have also been reported for NRs such as PPAR (*40*), LXR (*41*), or REV-ERBα and REV-ERBβ (*11, 12*). This suggests that the micromolar affinity of DHR51-LBD for heme is compatible with heme being its natural ligand.

Our UV−visible and EPR spectroscopy data, as well as the chemical modification experiments, establish that the heme bound to DHR51 contains a hexacoordinated low-spin ferric heme iron with axial cysteine and histidine ligands. The unchanged position of the Soret band (424 nm, Table 1) after reduction of the heme iron suggests that DHR51-LBD undergoes a redox-mediated ligand switch (*27*). The UV−visible spectrum of the CO and NO complexes reveals that the DHR51 heme-binding pocket is accessible to gas molecules. Similar to the other described Cys/His hemoproteins, such as HRI, CBS, NPAS2, Bach1, or E75, in the CO complex the thiolate ligand is replaced by a neutral amino acid, presumably a histidine (*42*). This is reflected by the position of the Soret band at 420 nm (Table 1). Dissociation of both heme iron protein ligands by NO was also observed with these proteins (there are no available data for Bach1).

In spite of the fact that the sequence homology between DHR51 and E75 LBDs is very low, except at positions conserved in all nuclear receptors (Figure 6), the metal coordination in these two NRs is very similar. This similarity is revealed by the spectra of the Fe(III), Fe(II), Fe(II)-NO, and Fe(II)-CO forms, which are identical for both nuclear receptors (*8*). This is in contrast with the data published on REV-ERBβ. The high resolution structure of this nuclear receptor (PDB ID 3CQV) present a His/Cys iron coordination, but it exhibits a Soret band around 415 nm for the oxidized form (*11, 12*).

Although DHR51 and E75 LBDs have a similar metal coordination, the binding mode of the heme is likely to be different in the two NRs. This is suggested by the following divergences. The affinities of DHR51 and E75 LBDs for the heme differ by several orders of magnitude (μM versus nM). Apo-DHR51-LBD seems more stable than apo-E75-LBD; the former was able to incorporate heme even after purification, whereas the latter could only bind heme either during protein expression or very shortly after cell lysis (*9*). The DHR51 histidine residue, corresponding to a position close to the heme iron ligand H574 of E75 (Figure 6), is not involved in heme binding, as indicated by site directed mutagenesis experiment.

Among the two types of nuclear receptors previously known to bind heme, E75 was proposed to be a gas sensor (*8*), and the REV-ERBs were shown not to be gas sensors (*11*). The characterization of the iron coordination presented here cannot be used to decide whether DHR51 is a gas or a heme sensor. Like DHR51-LBD, most of the heme-sensor proteins undergo redox-mediated ligand switch. However, the switch is unlikely to function as a signal because the resulting Fe(II) complex has been proposed to bind in a nonspecific manner to the protein (*43*). The replacement of the heme thiolate ligand by a neutral residue in the CO-complex and the absence of a sixth ligand in the NO-complex, observed with DHR51-LBD, have been described for both kinds of sensor proteins.

In terms of affinity, a gas sensor would be expected to exhibit high affinity for heme in order to keep it tightly bound. The micromolar affinity of DHR51 for heme suggests that it is more likely a heme sensor. As a matter of comparison, the heme responsive transcription factor Bach1 and the NRs REV-ERBα and REV-ERBβ display K_d values of 0.1 μM and 2−3 μM, respectively (*11, 12, 44*). There are exceptions to this concept as the two heme sensors, HRI and

the isolated PAS-A domain of NPAS2, have low K_d values of about 10^{-10} M (*45, 46*).

Considering that nothing is known about the gene target of DHR51, the data reported here should provide a starting point for new investigations. Like its human and *C. elegans* orphan homologues PNR and FAX-1 (*14, 47*), DHR51 is proposed to be involved in the regulation of neuron identity. Along these lines, heme deficiency has been reported to suppress the expression of key neuronal genes, causing an alteration of the proper functioning of neuronal cells (*48*).

ACKNOWLEDGMENT

We thank the Université Joseph Fourier (Grenoble, France) students Daniela Zaad and Morgane Bergada-Gala for a significant contribution to this work, and Delphine Blot and Christophe Guérin for technical assistance. We are grateful to Jacques Gaillard (CEA, Grenoble, France) for the EPR experiments and helpful discussions, to Nadia Izadi-Pruneyre (Institut Pasteur, Paris, France) for providing us with the HasA protein, and to Anne Imberty (CERMAV, Grenoble, France) for her invaluable help with the ITC experiments.

SUPPORTING INFORMATION AVAILABLE

Sequence of oligonucleotides used to clone the NR LBDs and the resultant protein sequences; differences between the DH51 and DHR83 cloned sequences and predicted sequences; and spectroscopic data on untagged-DHR51, DHR83, HNF4, and E75 LBDs. This material is available free of charge via the Internet at http://pubs.acs.org.

REFERENCES

1. Francis, G. A., Fayard, E., Picard, F., and Auwerx, J. (2003) Nuclear receptors and the control of metabolism. *Annu. Rev. Physiol. 65*, 261–311.
2. Bain, D. L., Heneghan, A. F., Connaghan-Jones, K. D., and Miura, M. T. (2007) Nuclear receptor structure: implications for function. *Annu. Rev. Physiol. 69*, 201–220.
3. Renaud, J. P., and Moras, D. (2000) Structural studies on nuclear receptors. *Cell. Mol. Life Sci. 57*, 1748–1769.
4. King-Jones, K., and Thummel, C. S. (2005) Nuclear receptors-a perspective from Drosophila. *Nat. Rev. Genet. 6*, 311–323.
5. Clayton, G. M., Peak-Chew, S. Y., Evans, R. M., and Schwabe, J. W. (2001) The structure of the ultraspiracle ligand-binding domain reveals a nuclear receptor locked in an inactive conformation. *Proc. Natl. Acad. Sci. U.S.A. 98*, 1549–1554.
6. Baker, K. D., Shewchuk, L. M., Kozlova, T., Makishima, M., Hassell, A., Wisely, B., Caravella, J. A., Lambert, M. H., Reinking, J. L., Krause, H., Thummel, C. S., Willson, T. M., and Mangelsdorf, D. J. (2003) The Drosophila orphan nuclear receptor DHR38 mediates an atypical ecdysteroid signaling pathway. *Cell 113*, 731–742.
7. Billas, I. M., Iwema, T., Garnier, J. M., Mitschler, A., Rochel, N., and Moras, D. (2003) Structural adaptability in the ligand-binding pocket of the ecdysone hormone receptor. *Nature 426*, 91–96.
8. Reinking, J., Lam, M. M., Pardee, K., Sampson, H. M., Liu, S., Yang, P., Williams, S., White, W., Lajoie, G., Edwards, A., and Krause, H. M. (2005) The Drosophila nuclear receptor e75 contains heme and is gas responsive. *Cell 122*, 195–207.
9. de Rosny, E., de Groot, A., Jullian-Binard, C., Gaillard, J., Borel, F., Pebay-Peyroula, E., Fontecilla-Camps, J. C., and Jouve, H. M. (2006) Drosophila nuclear receptor E75 is a thiolate hemoprotein. *Biochemistry 45*, 9727–9734.
10. White, K. P., Hurban, P., Watanabe, T., and Hogness, D. S. (1997) Coordination of Drosophila metamorphosis by two ecdysone-induced nuclear receptors. *Science 276*, 114–117.
11. Raghuram, S., Stayrook, K. R., Huang, P., Rogers, P. M., Nosie, A. K., McClure, D. B., Burris, L. L., Khorasanizadeh, S., Burris, T. P., and Rastinejad, F. (2007) Identification of heme as the ligand for the orphan nuclear receptors REV-ERBalpha and REV-ERBbeta. *Nat Struct Mol Biol 14*, 1207–1213.
12. Yin, L., Wu, N., Curtin, J. C., Qatanani, M., Szwergold, N. R., Reid, R. A., Waitt, G. M., Parks, D. J., Pearce, K. H., Wisely, G. B., and Lazar, M. A. (2007) Rev-erbalpha, a heme sensor that coordinates metabolic and circadian pathways. *Science 318*, 1786–1789.
13. Adams, M. D., Celniker, S. E., Holt, R. A., Evans, C. A., Gocayne, J. D., Amanatides, P. G., Scherer, S. E., Li, P. W., Hoskins, R. A., Galle, R. F., George, R. A., Lewis, S. E., Richards, S., Ashburner, M., Henderson, S. N., Sutton, G. G., Wortman, J. R., Yandell, M. D., Zhang, Q., Chen, L. X., Brandon, R. C., Rogers, Y. H., Blazej, R. G., Champe, M., Pfeiffer, B. D., Wan, K. H., Doyle, C., Baxter, E. G., Helt, G., Nelson, C. R., Gabor, G. L., Abril, J. F., Agbayani, A., An, H. J., Andrews-Pfannkoch, C., Baldwin, D., Ballew, R. M., Basu, A., Baxendale, J., Bayraktaroglu, L., Beasley, E. M., Beeson, K. Y., Benos, P. V., Berman, B. P., Bhandari, D., Bolshakov, S., Borkova, D., Botchan, M. R., Bouck, J., Brokstein, P., Brottier, P., Burtis, K. C., Busam, D. A., Butler, H., Cadieu, E., Center, A., Chandra, I., Cherry, J. M., Cawley, S., Dahlke, C., Davenport, L. B., Davies, P., de Pablos, B., Delcher, A., Deng, Z., Mays, A. D., Dew, I., Dietz, S. M., Dodson, K., Doup, L. E., Downes, M., Dugan-Rocha, S., Dunkov, B. C., Dunn, P., Durbin, K. J., Evangelista, C. C., Ferraz, C., Ferriera, S., Fleischmann, W., Fosler, C., Gabrielian, A. E., Garg, N. S., Gelbart, W. M., Glasser, K., Glodek, A., Gong, F., Gorrell, J. H., Gu, Z., Guan, P., Harris, M., Harris, N. L., Harvey, D., Heiman, T. J., Hernandez, J. R., Houck, J., Hostin, D., Houston, K. A., Howland, T. J., Wei, M. H., Ibegwam, C., et al. (2000) The genome sequence of Drosophila melanogaster. *Science 287*, 2185–2195.
14. Milam, A. H., Rose, L., Cideciyan, A. V., Barakat, M. R., Tang, W. X., Gupta, N., Aleman, T. S., Wright, A. F., Stone, E. M., Sheffield, V. C., and Jacobson, S. G. (2002) The nuclear receptor NR2E3 plays a role in human retinal photoreceptor differentiation and degeneration. *Proc. Natl. Acad. Sci. U.S.A. 99*, 473–8.
15. de Groot, A., de Rosny, E., Juillan-Binard, C., Ferrer, J. L., Laudet, V., Pierce, R. J., Pebay-Peyroula, E., Fontecilla-Camps, J. C., and Borel, F. (2005) Crystal structure of a novel tetrameric complex of agonist-bound ligand-binding domain of Biomphalaria glabrata retinoid X receptor. *J. Mol. Biol. 354*, 841–853.
16. Beaven, G. H., Chen, S. H., d'Albis, A., and Gratzer, W. B. (1974) A spectroscopic study of the haemin−human-serum-albumin system. *Eur. J. Biochem. 41*, 539–546.
17. Deniau, C., Gilli, R., Izadi-Pruneyre, N., Letoffe, S., Delepierre, M., Wandersman, C., Briand, C., and Lecroisey, A. (2003) Thermodynamics of heme binding to the HasA(SM) hemophore: effect of mutations at three key residues for heme uptake. *Biochemistry 42*, 10627–10633.
18. Izadi, N., Henry, Y., Haladjian, J., Goldberg, M. E., Wandersman, C., Delepierre, M., and Lecroisey, A. (1997) Purification and characterization of an extracellular heme-binding protein, HasA, involved in heme iron acquisition. *Biochemistry 36*, 7050–7057.
19. Gouet, P., Jouve, H. M., and Dideberg, O. (1995) Crystal structure of Proteus mirabilis PR catalase with and without bound NADPH. *J. Mol. Biol. 249*, 933–954.
20. Cheesman, M. R., Little, P. J., and Berks, B. C. (2001) Novel heme ligation in a c-type cytochrome involved in thiosulfate oxidation: EPR and MCD of SoxAX from Rhodovulum sulfidophilum. *Biochemistry 40*, 10562–10569.
21. Dawson, J. H., Andersson, L. A., and Sono, M. (1982) Spectroscopic investigations of ferric cytochrome P-450-CAM ligand complexes. Identification of the ligand trans to cysteinate in the native enzyme. *J. Biol. Chem. 257*, 3606–3617.
22. Dhawan, I. K., Shelver, D., Thorsteinsson, M. V., Roberts, G. P., and Johnson, M. K. (1999) Probing the heme axial ligation in the CO-sensing CooA protein with magnetic circular dichroism spectroscopy. *Biochemistry 38*, 12805–12813.
23. Sigman, J. A., Pond, A. E., Dawson, J. H., and Lu, Y. (1999) Engineering cytochrome c peroxidase into cytochrome P450: a proximal effect on heme-thiolate ligation. *Biochemistry 38*, 11122–11129.
24. Konopka, K., and Waskell, L. (1988) Chemical modification of cytochrome b5, cytochrome c and myoglobin with diethylpyrocarbonate. *Biochim. Biophys. Acta 954*, 189–200.
25. Nakanishi, N., Takeuchi, F., Okamoto, H., Tamura, A., Hori, H., and Tsubaki, M. (2006) Characterization of heme-coordinating histidyl residues of cytochrome b5 based on the reactivity with diethylpyrocarbonate: a mechanism for the opening of axial imidazole rings. *J. Biochem. 140*, 561–71.

26. Miles, E. W. (1977) Modification of histidyl residues in proteins by diethylpyrocarbonate. *Methods Enzymol. 47*, 431–442.
27. Marvin, K. A., Kerby, R. L., Youn, H., Roberts, G. P., and Burstyn, J. N. (2008) The transcription regulator RcoM-2 from *Burkholderia xenovorans* is a cysteine-ligated hemoprotein that undergoes a redox-mediated ligand switch. *Biochemistry 47*, 9016–9028.
28. Pazicni, S., Lukat-Rodgers, G. S., Oliveriusova, J., Rees, K. A., Parks, R. B., Clark, R. W., Rodgers, K. R., Kraus, J. P., and Burstyn, J. N. (2004) The redox behavior of the heme in cystathionine beta-synthase is sensitive to pH. *Biochemistry 43*, 14684–14695.
29. Yoshioka, S., Takahashi, S., Hori, H., Ishimori, K., and Morishima, I. (2001) Proximal cysteine residue is essential for the enzymatic activities of cytochrome P450cam. *Eur. J. Biochem. 268*, 252–259.
30. Aono, S., Ohkubo, K., Matsuo, T., and Nakajima, H. (1998) Redox-controlled ligand exchange of the heme in the CO-sensing transcriptional activator CooA. *J. Biol. Chem. 273*, 25757–25764.
31. Igarashi, J., Sato, A., Kitagawa, T., Yoshimura, T., Yamauchi, S., Sagami, I., and Shimizu, T. (2004) Activation of heme-regulated eukaryotic initiation factor 2alpha kinase by nitric oxide is induced by the formation of a five-coordinate NO-heme complex: optical absorption, electron spin resonance, and resonance raman spectral studies. *J. Biol. Chem. 279*, 15752–15762.
32. Uchida, T., Sato, E., Sato, A., Sagami, I., Shimizu, T., and Kitagawa, T. (2005) CO-dependent activity-controlling mechanism of heme-containing CO-sensor protein, neuronal PAS domain protein 2. *J. Biol. Chem. 280*, 21358–21368.
33. Perera, R., Sono, M., Sigman, J. A., Pfister, T. D., Lu, Y., and Dawson, J. H. (2003) Neutral thiol as a proximal ligand to ferrous heme iron: implications for heme proteins that lose cysteine thiolate ligation on reduction. *Proc. Natl. Acad. Sci. U.S.A. 100*, 3641–3646.
34. Reynolds, M. F., Parks, R. B., Burstyn, J. N., Shelver, D., Thorsteinsson, M. V., Kerby, R. L., Roberts, G. P., Vogel, K. M., and Spiro, T. G. (2000) Electronic absorption, EPR, and resonance raman spectroscopy of CooA, a CO-sensing transcription activator from *R. rubrum*, reveals a five-coordinate NO-heme. *Biochemistry 39*, 388–396.
35. Yonetani, T., Yamamoto, H., Erman, J. E., Leigh, J. S., Jr., and Reed, G. H. (1972) Electromagnetic properties of hemoproteins. V. Optical and electron paramagnetic resonance characteristics of nitric oxide derivatives of metalloporphyrin-apohemoprotein complexes. *J. Biol. Chem. 247*, 2447–2455.
36. Derbyshire, E. R., Gunn, A., Ibrahim, M., Spiro, T. G., Britt, R. D., and Marletta, M. A. (2008) Characterization of two different five-coordinate soluble guanylate cyclase ferrous-nitrosyl complexes. *Biochemistry 47*, 3892–3899.
37. Mense, S. M., and Zhang, L. (2006) Heme: a versatile signaling molecule controlling the activities of diverse regulators ranging from transcription factors to MAP kinases. *Cell Res. 16*, 681–692.
38. Shelver, D., Kerby, R. L., He, Y., and Roberts, G. P. (1997) CooA, a CO-sensing transcription factor from *Rhodospirillum rubrum*, is a CO-binding heme protein. *Proc. Natl. Acad. Sci. U.S.A. 94*, 11216–11220.
39. Palanker, L., Necakov, A. S., Sampson, H. M., Ni, R., Hu, C., Thummel, C. S., and Krause, H. M. (2006) Dynamic regulation of Drosophila nuclear receptor activity in vivo. *Development 133*, 3549–3562.
40. Krey, G., Braissant, O., L'Horset, F., Kalkhoven, E., Perroud, M., Parker, M. G., and Wahli, W. (1997) Fatty acids, eicosanoids, and hypolipidemic agents identified as ligands of peroxisome proliferator-activated receptors by coactivator-dependent receptor ligand assay. *Mol. Endocrinol. 11*, 779–791.
41. Janowski, B. A., Grogan, M. J., Jones, S. A., Wisely, G. B., Kliewer, S. A., Corey, E. J., and Mangelsdorf, D. J. (1999) Structural requirements of ligands for the oxysterol liver X receptors LXRalpha and LXRbeta. *Proc. Natl. Acad. Sci. U.S.A. 96*, 266–271.
42. Igarashi, J., Kitanishi, K., Martinkova, M., Murase, M., Iizuka, A., and Shimizu, T. (2008) The Roles of thiolate-heme proteins, other than the P450 cytochromes in the regulation of heme-sensor proteins. *Acta Chim. Slov.* 67–74.
43. Igarashi, J., Murase, M., Iizuka, A., Pichierri, F., Martinkova, M., and Shimizu, T. (2008) Elucidation of the heme binding site of heme-regulated eukaryotic initiation factor 2alpha kinase and the role of the regulatory motif in heme sensing by spectroscopic and catalytic studies of mutant proteins. *J. Biol. Chem. 283*, 18782–18791.
44. Ogawa, K., Igarashi, K., Nishitani, C., Shibahara, S., and Fujita, H. (2002) Heme-regulated transcription factor Bach1. *J. Health Sci. 48*, 1–6.
45. Miksanova, M., Igarashi, J., Minami, M., Sagami, I., Yamauchi, S., Kurokawa, H., and Shimizu, T. (2006) Characterization of heme-regulated eIF2alpha kinase: roles of the N-terminal domain in the oligomeric state, heme binding, catalysis, and inhibition. *Biochemistry 45*, 9894–9905.
46. Mukaiyama, Y., Uchida, T., Sato, E., Sasaki, A., Sato, Y., Igarashi, J., Kurokawa, H., Sagami, I., Kitagawa, T., and Shimizu, T. (2006) Spectroscopic and DNA-binding characterization of the isolated heme-bound basic helix-loop-helix-PAS-A domain of neuronal PAS protein 2 (NPAS2), a transcription activator protein associated with circadian rhythms. *FEBS J. 273*, 2528–2539.
47. Wightman, B., Ebert, B., Carmean, N., Weber, K., and Clever, S. (2005) The *C. elegans* nuclear receptor gene fax-1 and homeobox gene unc-42 coordinate interneuron identity by regulating the expression of glutamate receptor subunits and other neuron-specific genes. *Dev. Biol. 287*, 74–85.
48. Sengupta, A., Hon, T., and Zhang, L. (2005) Heme deficiency suppresses the expression of key neuronal genes and causes neuronal cell death. *Brain Res. Mol. Brain Res. 137*, 23–30.
49. Brelivet, Y., Kammerer, S., Rochel, N., Poch, O., and Moras, D. (2004) Signature of the oligomeric behaviour of nuclear receptors at the sequence and structural level. *EMBO Rep. 5*, 423–429.

BI801691B